The Ehrenfest method with fully quantum nuclear motion (Qu-Eh): Application to charge migration in radical cations

Andrew J. Jenkins, K. Eryn Spinlove, Morgane Vacher, Graham A. Worth, and Michael A. Robb

Citation: The Journal of Chemical Physics **149**, 094108 (2018); doi: 10.1063/1.5038428
View online: https://doi.org/10.1063/1.5038428
View Table of Contents: http://aip.scitation.org/toc/jcp/149/9
Published by the American Institute of Physics

The Ehrenfest method with fully quantum nuclear motion (Qu-Eh): Application to charge migration in radical cations

Andrew J. Jenkins,[1] K. Eryn Spinlove,[2] Morgane Vacher,[3] Graham A. Worth,[2] and Michael A. Robb[4]

[1]*Department of Chemistry, University of Washington, Seattle, Washington 98195, USA*
[2]*Department of Chemistry, University College London, 20, Gordon St., WC1H 0AJ London, United Kingdom*
[3]*Department of Chemistry-Ångström, Uppsala University, Lägerhyddsvägen 1, 751 21 Uppsala, Sweden*
[4]*Department of Chemistry, Imperial College London, London SW7 2AZ, United Kingdom*

(Received 3 May 2018; accepted 21 August 2018; published online 7 September 2018)

An algorithm is described for quantum dynamics where an Ehrenfest potential is combined with fully quantum nuclear motion (Quantum-Ehrenfest, Qu-Eh). The method is related to the single-set variational multi-configuration Gaussian approach (vMCG) but has the advantage that only a single quantum chemistry computation is required at each time step since there is only a single time-dependent potential surface. Also shown is the close relationship to the "exact factorization method." The quantum Ehrenfest method is compared with vMCG for study of electron dynamics in a modified bismethylene-adamantane cation system. Illustrative examples of electron-nuclear dynamics are presented for a distorted allene system and for $HCCI^+$ where one has a degenerate Π system.
https://doi.org/10.1063/1.5038428

I. INTRODUCTION

Nonadiabatic dynamics[1] is becoming an essential tool for the investigation of chemical processes that involve more than one potential surface, as occurs in photochemistry. Many nonadiabatic dynamics methods in current use treat the electronic structure using quantum chemistry but use classical trajectories to represent nuclear motion. However, since in most cases one must change the electronic state along a reaction coordinate, it is desirable to use quantum dynamics for the nuclear motion to retain the nuclear coherence. Quantum dynamics methods use adiabatic potential surfaces (although the dynamics is performed on diabatic surfaces). However, in the case where a coherent superposition[2] of electronic states is created in an experiment, the dynamics occurs on a potential that does not correspond to a single Born-Oppenheimer surface. This paper focuses on a practical approach for this more general type of problem where the electron and nuclear motion can be asynchronous.

The use of Gaussian wavepackets (gwp), where centroids of the Gaussians are tied to trajectories (quantum trajectories), which have, in turn, been determined by solving the time dependent Schrödinger equation (TDSE), is a useful practical approach to quantum dynamics.[1,3–5] The direct dynamics variational multiconfiguration Gaussian (DD-vMCG) method[1,3,5–7] is one example of a class of *on-the-fly* quantum dynamics methods in which the potential surfaces are calculated as required for the propagation using electronic structure computations. Other approaches can be found in developments of Martinez and co-workers on the "multiple spawning" method[8,9] which use classical trajectories and the "exact factorization" approaches of Gross[10–12] and Cederbaum.[13] The equations for DD-vMCG[1,3,6,7] use a local harmonic representation of each electronic state and thus require first and second derivatives of the potential energies derived from electronic structure computations at points along the quantum trajectories. Thus, they can be used with any method for which such energy derivatives can be obtained. If more than one electronic state is considered, then diabatic potential surfaces are used and time evolution of the amplitude coefficients of the diabatic states is obtained from the TDSE.

In "single-set" DD-vMCG, the nuclear motion is represented by one set of fully coherent gwp, which follow "quantum" trajectories. Each gwp has different amplitude coefficients for each electronic state along a given trajectory. (The other possibility is multi-set where each potential surface has its own set of gwp, but this approach is not stable in practice). There are two types of equations of motion:[3] the first gives the time evolution of the expansion coefficients with respect to the electronic state and the gwp, while the second gives the time evolution of the mean positions and momenta of the gwp. The initial conditions and dynamics are formulated in DD-vMCG in terms of diabatic states, which are usually formed from a set of adiabatic states. One quantum chemistry computation is required for every electronic adiabatic state at each time step in DD-vMCG.

If the gwp are chosen to follow classical trajectories then one has the multi-configuration Ehrenfest method[14–17] or the *Ab Inito* Multiple Spawning (AIMS) method.[8,9] In these methods, the trajectories are coupled via time evolution of the expansion coefficients of the gwp. The traditional Ehrenfest

method has the additional approximation that the trajectories are independent and decoupled and hence no transfer of population among the individual trajectories is possible. In this case the TDSE is used for the electronic degrees of motion only.

The underlying principles of the Ehrenfest implementation used in this work can be found in Vacher *et al.*[18] where a comparison with DD-vMCG is made. In that paper, we showed that an Ehrenfest method could be derived as a special case of single-set DD-vMCG, in the limit of a single (time-dependent) potential surface, where the nuclei are constrained to move classically. The first and second derivatives of the energy of the Ehrenfest wavefuction can also be determined.[19] The gradients and Hessian with respect to nuclear motion[19] require the full general formulation of Almlöf and Taylor[20] since the wavefunction is not an optimized eigenstate.

Within the Ehrenfest type approaches there are three possible ways to describe the motion of a nuclear wavepacket: (i) with an ensemble of independent trajectories that move classically according to the Ehrenfest force,[18] (ii) with Gaussian functions floating on the classical trajectories and their expansion coefficients propagated and coupled via the TDSE, thus allowing for transfer of population between the trajectories,[14–17,21] or (iii) with Gaussian functions that move according to the TDSE. This paper focuses on an algorithmic formulation of (iii) which we shall call Quantum Ehrenfest (Qu-Eh). Here, the nuclear motion obeys quantum mechanics as in single-set DD-vMCG, but on a single effective time-dependent potential energy surface that corresponds to the Ehrenfest wavefunction.

II. THEORETICAL METHOD: THE QUANTUM EHRENFEST METHOD (Qu-Eh)

The Quantum Ehrenfest method can be derived as a variation of the DD-vMCG approach with a global time-dependent potential. The starting point is the exact factorization of the full wavefunction

$$\Psi(\mathbf{q},\mathbf{r},t) = \chi(\mathbf{q},t)\psi(\mathbf{r},t;\mathbf{q}), \tag{1}$$

where $\mathbf{q}$ are the nuclear coordinates, $\mathbf{r}$ the electronic coordinates, and $\psi(\mathbf{r},t;\mathbf{q})$ reminds us that there is an electronic wavefunction for each nuclear configuration $\mathbf{q}$. As shown by Gross and co-workers,[11] this ansatz is completely general. To make a practical propagation method, we now follow the DD-vMCG approach and expand the nuclear wavefunction, χ, in a set of time-dependent gwp $\{g_i\}$,

$$\chi(\mathbf{q},t) = \sum_i A_i(t) g_i(\mathbf{q},t) \tag{2}$$

which results in the following ansatz for the full wavefunction:

$$\Psi(\mathbf{q},\mathbf{r},t) = \sum_i A_i(t) g_i(\mathbf{q},t)\psi(\mathbf{r},t;\mathbf{q}). \tag{3}$$

The Dirac-Frenkel Variational Principle

$$\langle \delta\Psi | H - i\frac{\partial}{\partial t} | \Psi\rangle = 0 \tag{4}$$

is then used to solve the TDSE using the ansatz (3). (Note that we use atomic units throughout.)

First, one of the expansion coefficients is varied, $\delta\Psi = g_k\psi\delta A_k$ which leads to

$$i\sum_j \langle \psi g_i | g_j\psi\rangle \dot{A}_j = \sum_j \Big(\langle \psi g_i | H | g_j\psi\rangle - i\langle \psi g_i | \dot{g}_j\psi\rangle - i\langle \psi g_i | g_j\dot{\psi}\rangle \Big) A_j. \tag{5}$$

In this equation, and the following, the $\langle \cdots | \cdots \rangle$ notation is used to indicate that the scalar product represents the integration over all the variables inside the brackets. In the exact factorization ansatz, a key property is that the electronic wavefunction is, and remains, normalised at every nuclear configuration, i.e.,

$$\langle \psi | \psi \rangle = 1 \tag{6}$$

and

$$i\langle \psi | \dot{\psi}\rangle = \Theta(\mathbf{q}), \tag{7}$$

where Θ is an arbitrary $\mathbf{q}$-dependent real function. The equation of motion for the expansion coefficients can now be written as

$$i\dot{A}_k = \sum_{ij} S^{-1}_{ki} \Big(H_{ij} - i\tau_{ij} - T_{ij} \Big) A_j, \tag{8}$$

where

$$\begin{aligned} H_{ij} &= \langle g_i\psi | H | g_j\psi\rangle, \;\; S_{ij} = \langle g_i | g_j\rangle, \\ \tau_{ij} &= \langle g_i | \dot{g}_j\rangle, \;\; T_{ij} = \langle g_i | \Theta | g_j\rangle, \end{aligned} \tag{9}$$

i.e., $\mathbf{S}$ is the gwp overlap matrix, τ the time-derivative overlap matrix, and $\mathbf{T}$ the matrix of Θ in the gwp basis.

The gwp g_i is described by a set of time-dependent parameters λ_i. The αth parameter of the ith gwp is then varied as $\delta\Psi = \delta\lambda_{\alpha i}\frac{\partial g_i}{\partial \lambda_{\alpha i}}\psi A_i$ to give

$$\begin{aligned} i\sum_{j\beta} A^*_i \langle \psi \frac{\partial g_i}{\partial \lambda_{\alpha i}} | \frac{\partial g_j}{\partial \lambda_{\beta j}}\psi\rangle A_j \dot{\lambda}_{\beta j} = {} & \sum_j A^*_i \langle \psi \frac{\partial g_i}{\partial \lambda_{\alpha i}} | H | g_j\psi\rangle A_j \\ & - iA^*_i \langle \psi \frac{\partial g_i}{\partial \lambda_{\alpha i}} | g_j\psi\rangle \dot{A}_j \\ & - iA^*_i \langle \psi \frac{\partial g_i}{\partial \lambda_{\alpha i}} | g_j\dot{\psi}\rangle A_j. \end{aligned} \tag{10}$$

Substituting for $\dot{A}_j$ with Eq. (8) and again applying the normalisation condition of the electronic wavefunction results in equations of motion for the Gaussian parameters that look like the DD-vMCG equations, except for the additional factors dependent on the function Θ,

$$i\dot{\lambda}_{\beta k} = \sum_{\alpha ij} C^{-1}_{\beta k \alpha i}\rho_{ij}\left(H^{(\alpha 0)}_{ij} - T^{(\alpha 0)}_{ij} - \sum_{lm} S^{(\alpha 0)}_{il} S^{-1}_{lm} \Big(H_{mj} - T_{mj} \Big) \right). \tag{11}$$

Here we have the usual DD-vMCG C-matrix

$$C_{\alpha i \beta j} = \rho_{ij}\left(S^{(\alpha\beta)}_{ij} - \sum_{lm} S^{(\alpha 0)}_{kl} S^{-1}_{lm} S^{(0\beta)}_{mj} \right), \tag{12}$$

the Hamiltonian matrices

$$H^{(\alpha 0)}_{ij} = \langle \frac{\partial g_i}{\partial \lambda_{\alpha i}}\psi | H | g_j\psi\rangle, \tag{13}$$

the density matrix

$$\rho_{ij} = A_i^* A_j, \tag{14}$$

and the derivative overlap matrices and the derivative electronic wavefunction matrix

$$S_{ij}^{(\alpha 0)} = \langle \frac{\partial g_i}{\partial \lambda_{\alpha i}} | g_j \rangle, \quad S_{ij}^{(\alpha\beta)} = \langle \frac{\partial g_i}{\partial \lambda_{\alpha i}} | \frac{\partial g_j}{\partial \lambda_{\beta j}} \rangle, \quad T_{ij}^{(\alpha 0)} = \langle \frac{\partial g_i}{\partial \lambda_{\alpha i}} | \Theta | g_j \rangle. \tag{15}$$

Finally, the electronic wavefunction at a particular nuclear configuration, $\mathbf{q}$, is varied as $\delta\Psi = \sum_i A_i g_i(\mathbf{q}) \delta\psi(\mathbf{q})$ giving

$$i \sum_{ij} A_i^* \langle g_i | g_j \rangle_{\mathbf{q}} A_j |\dot{\psi}\rangle_{\mathbf{q}} = \left(\sum_{ij} A_i^* \langle g_i | H | g_j \rangle_{\mathbf{q}} A_j - i A_i^* \langle g_i | \dot{g}_j \rangle_{\mathbf{q}} A_j - i A_i^* \langle g_i | g_j \rangle_{\mathbf{q}} \dot{A}_j \right) |\psi\rangle_{\mathbf{q}}, \tag{16}$$

where $\langle \cdots | \cdots \rangle_{\mathbf{q}}$ indicates that this scalar product is evaluated at the nuclear configuration $\mathbf{q}$ rather than integrating over the nuclear coordinates. For example,

$$S_{ij}(\mathbf{q}) = \langle g_i | g_j \rangle_{\mathbf{q}} = g_i^*(\mathbf{q}) g_j(\mathbf{q}) \tag{17}$$

is the product of the gwp values at $\mathbf{q}$. From the nuclear wavefunction ansatz, (2), the nuclear density at $\mathbf{q}$ is given by

$$\rho(\mathbf{q}) = \langle \chi | \chi \rangle_{\mathbf{q}} = \sum_{ij} A_i^* \langle g_i | g_j \rangle_{\mathbf{q}} A_j = \sum_{ij} A_i^* S_{ij}(\mathbf{q}) A_j, \tag{18}$$

and as, from Eq. (8),

$$i \sum_{ij} A_i^* S_{ij} \dot{A}_j + i A_i^* \tau_{ij} A_j = \sum_{ij} A_i^* H_{ij} A_j - A_i^* T_{ij} A_j, \tag{19}$$

it can be taken that at each nuclear configuration

$$\langle \chi | \dot{\chi} \rangle_{\mathbf{q}} = \sum_{ij} A_i^* \langle g_i | g_j \rangle_{\mathbf{q}} \dot{A}_j + A_i^* \langle g_i | \dot{g}_j \rangle_{\mathbf{q}} A_j = \sum_{ij} A_i^* H_{ij}(\mathbf{q}) A_j - A_i^* T_{ij}(\mathbf{q}) A_j, \tag{20}$$

where $H_{ij}(\mathbf{q})$ and $S_{ij}(\mathbf{q})$ are the Hamiltonian matrix elements and gwp overlap matrix evaluated at the nuclear configuration $\mathbf{q}$. Note that the matrix $H_{ij}(\mathbf{q})$ is not Hermitian. Substituting Eqs. (18) and (20) into Eq. (16) gives

$$i|\dot{\psi}\rangle_{\mathbf{q}} = [\rho(\mathbf{q})]^{-1} \left(\sum_{ij} A_i^* H_{ij}^g(\mathbf{q}) A_j - A_i^* H_{ij}(\mathbf{q}) A_j + A_i^* T_{ij}(\mathbf{q}) A_j \right) |\psi\rangle_{\mathbf{q}}, \tag{21}$$

where

$$H_{ij}^g(\mathbf{q}) = \langle g_i | H | g_j \rangle_{\mathbf{q}} \tag{22}$$

defines the Hamiltonian matrix in the Gaussian basis set evaluated at the configuration $\mathbf{q}$. This is an operator on the electronic function at this point.

To summarize, the equations of motion Eqs. (8), (11), and (21) form a coupled set of equations of motion for the expansion coefficients, gwp nuclear basis functions, and time-dependent electronic function. Collecting these equations together,

$$i\dot{A}_k = \sum_{ij} S_{ki}^{-1} \left(H_{ij} - i\tau_{ij} - T_{ij} \right) A_j, \tag{23}$$

$$i\dot{\lambda}_{\beta k} = \sum_{\alpha ij} C_{\beta k \alpha i}^{-1} \rho_{ij} \left(H_{ij}^{(\alpha 0)} - T_{ij}^{(\alpha 0)} - \sum_{lm} S_{il}^{(\alpha 0)} S_{lm}^{-1} \left(H_{mj} - T_{mj} \right) \right), \tag{24}$$

$$i|\dot{\psi}\rangle_{\mathbf{q}} = [\rho(\mathbf{q})]^{-1} \left(\sum_{ij} A_i^* H_{ij}^g(\mathbf{q}) A_j - A_i^* H_{ij}(\mathbf{q}) A_j + A_i^* T_{ij}(\mathbf{q}) A_j \right) |\psi\rangle_{\mathbf{q}}. \tag{25}$$

The function Θ controls the relative phases of the parts of the evolving equations and is still undefined. Consequently, the final step is to explicitly expand the Hamiltonian matrices to show the nature of the coupling and to choose the function Θ to simplify the equations. Writing the Hamiltonian in the usual way as a sum of nuclear kinetic energy operator, T_N, and electronic Hamiltonian that depends on the nuclear configuration, $H_{\mathrm{el}}(\mathbf{q})$, the Hamiltonian matrix elements at a particular configuration are

$$H_{ij}(\mathbf{q}) = \langle g_i \psi | T_N + H_{\mathrm{el}} | g_j \psi \rangle_{\mathbf{q}} \tag{26}$$

$$= g_i^*(\mathbf{q}) \langle \psi | T_N | \psi \rangle_{\mathbf{q}} g_j(\mathbf{q}) + S_{ij}(\mathbf{q}) V(\mathbf{q}), \tag{27}$$

where we introduce the time-dependent Ehrenfest potential

$$V(\mathbf{q}) = \langle \psi | H_{\mathrm{el}} | \psi \rangle_{\mathbf{q}} \tag{28}$$

which is a global surface defined by the motion of the nuclei via the evolution of the electronic function Eq. (25). If the system is described with mass-scaled coordinates so that $T_N = -\frac{1}{2}\vec{\nabla} \cdot \vec{\nabla}$, then

$$\langle \psi | T_N | \psi \rangle_{\mathbf{q}} = -\frac{1}{2} \vec{\nabla}^2 - \langle \psi | \vec{\nabla} \psi \rangle_{\mathbf{q}} \cdot \vec{\nabla} - \frac{1}{2} \langle \psi | \vec{\nabla}^2 \psi \rangle_{\mathbf{q}} \tag{29}$$

$$= T_N + 2\vec{F}(\mathbf{q}) \cdot \vec{\nabla} + G(\mathbf{q}), \tag{30}$$

where the second line defines the vector derivative term, $\vec{F}(\mathbf{q})$, and the scalar derivative term, $G(\mathbf{q})$. Thus the Hamiltonian matrix elements can be written as

$$H_{ij}(\mathbf{q}) = \langle g_i | T_N g_j \rangle_{\mathbf{q}} + 2\vec{F}(\mathbf{q}) \cdot \langle g_i | \vec{\nabla} g_j \rangle_{\mathbf{q}} + S_{ij}(\mathbf{q}) G(\mathbf{q}) + S_{ij}(\mathbf{q}) V(\mathbf{q}) \tag{31}$$

with the second term coupling the electronic motion to the nuclear momentum via an Ehrenfest derivative coupling, and the third term is an Ehrenfest non-adiabatic correction to the Ehrenfest potential. In a similar way, the Hamiltonian matrix operator in terms of just the gwp basis is

$$H_{ij}^g(\mathbf{q}) = \langle g_i | T_N + H_{\mathrm{el}}(\mathbf{q}) | g_j \rangle_{\mathbf{q}} \tag{32}$$

$$= \langle g_i | T_N g_j \rangle_{\mathbf{q}} - \langle g_i | \vec{\nabla} g_j \rangle_{\mathbf{q}} . \vec{\nabla} - \frac{1}{2} S_{ij}(\mathbf{q}) \nabla^2 + S_{ij}(\mathbf{q}) H_{\mathrm{el}}(\mathbf{q}). \tag{33}$$

Various choices for Θ can be made. It can be set to zero or, in line with the usual Ehrenfest approach, set to be the electronic energy. Here, we shall set it equal to the real number

$$\begin{aligned}\boldsymbol{\Theta}(\mathbf{q}) &= 2\sum_{ij} A_i^* \frac{\vec{F}(\mathbf{q})\cdot\langle g_i|\vec{\nabla}g_j\rangle_{\mathbf{q}}}{\rho(\mathbf{q})}A_j + G(\mathbf{q}) \\ &= 2\mathcal{F}(\mathbf{q}) + G(\mathbf{q}),\end{aligned} \tag{34}$$

where the second equation on the RHS defines the function $\mathcal{F}$. This choice leads to DD-vMCG-like equations of motion for the expansion coefficients and gwp parameters,

$$i\dot{A}_k = \sum_{ij} S^{-1}_{ki}\left(H^N_{ij} - i\tau_{ij}\right)A_j, \tag{35}$$

$$i\dot{\lambda}_{\beta k} = \sum_{\alpha ij} C^{-1}_{\beta k\alpha i}\rho_{ij}\left(H^{N(\alpha 0)}_{ij} - \sum_{lm} S^{(\alpha 0)}_{il}S^{-1}_{lm}H^N_{mj}\right). \tag{36}$$

Here we have defined a nuclear Hamiltonian, H^N, which has matrix elements

$$H^N_{ij} = \langle g_i|T_N g_j\rangle + \langle g_i|V|g_j\rangle + 2\vec{F}(\mathbf{q})\cdot\langle g_i|\vec{\nabla}g_j\rangle - 2\mathcal{F}(\mathbf{q}). \tag{37}$$

For the electronic functions, this results in

$$\begin{aligned}i|\dot{\psi}\rangle_{\mathbf{q}} &= [\rho(\mathbf{q})]^{-1}\Bigg(\sum_{ij} -A_i^*\langle g_i|\vec{\nabla}g_j\rangle_{\mathbf{q}}A_j\cdot\vec{\nabla} - \frac{1}{2}A_i^*S_{ij}A_j(\mathbf{q})\nabla^2 \\ &\quad + A_i^*S_{ij}(\mathbf{q})H_{\mathrm{el}}(\mathbf{q})A_j - A_i^*\langle g_i|V|g_j\rangle_{\mathbf{q}}A_j\Bigg)|\psi\rangle_{\mathbf{q}}\end{aligned} \tag{38}$$

$$= \left(H_{\mathrm{el}}(\mathbf{q}) - V(\mathbf{q}) - \frac{1}{2}\nabla^2 + [\rho(\mathbf{q})]^{-1}i\vec{p}(\mathbf{q})\cdot\vec{\nabla}\right)|\psi\rangle_{\mathbf{q}}, \tag{39}$$

where the nuclear momentum at $\mathbf{q}$ is

$$\vec{p}(\mathbf{q}) = -i\sum_{ij} A_i^*\langle g_i|\vec{\nabla}g_j\rangle_{\mathbf{q}}A_j = -i\langle\chi|\vec{\nabla}\chi\rangle_{\mathbf{q}}. \tag{40}$$

Equations (35), (36), and (38) are still an exact reformulation of the TDSE. These equations are, however, difficult to solve due to the appearance of the Ehrenfest derivative coupling in the equations of motion for the expansion coefficients, along with the nuclear coordinate derivative operator in the evolution of the electronic functions. It is informative to expand the electronic wavefunction in a basis set of orthonormal time-independent electronic functions, $\{\psi_s\}$, at a fixed nuclear geometry,

$$|\psi\rangle = \sum_s c_s(t)|\psi_s\rangle. \tag{41}$$

Using this expansion, Eq. (38) can be written as

$$\begin{aligned}i\langle\psi_s|\dot{\psi}\rangle_{\mathbf{q}} &= \sum_t \Bigg(\langle\psi_s|H_{\mathrm{el}}(\mathbf{q})|\psi_t\rangle - \delta_{st}V(\mathbf{q}) - \frac{1}{2}\langle\psi_s|\nabla^2\psi_t\rangle_{\mathbf{q}} \\ &\quad + [\rho(\mathbf{q})]^{-1}i\vec{p}(\mathbf{q})\cdot\langle\psi_s|\vec{\nabla}\psi_t\rangle_{\mathbf{q}}\Bigg)c_t\end{aligned} \tag{42}$$

and using the orthonormality of the basis,

$$\begin{aligned}i\dot{c}_s &= \sum_t \Bigg(H_{\mathrm{el},st}(\mathbf{q}) - \delta_{st}V(\mathbf{q}) - \frac{1}{2}G_{st}(\mathbf{q}) \\ &\quad + [\rho(\mathbf{q})]^{-1}i\vec{p}(\mathbf{q})\cdot\vec{D}_{st}(\mathbf{q})\Bigg)c_t,\end{aligned} \tag{43}$$

with the derivative coupling matrices

$$\vec{D}_{st}(\mathbf{q}) = \langle\psi_s|\vec{\nabla}\psi_t\rangle_{\mathbf{q}}, \quad G_{st}(\mathbf{q}) = \langle\psi_s|\nabla^2\psi_t\rangle_{\mathbf{q}}. \tag{44}$$

The matrix $\vec{D}$ is a form of non-adiabatic coupling that couples states s and t via the nuclear momentum, $\boldsymbol{p}$. A similar term arises in the equations for exact factorization.[10–12] It can be neglected in our computations because our Ehrenfest wavefunction is constructed in a full CI complete active space self-consistent field (CASSCF) (with diabatic basis) space. Thus we take the approximation

$$\vec{D}_{st}(\mathbf{q}) = 0. \tag{45}$$

This means, furthermore, that the matrix $\mathbf{G}$ is also zero, as is the Ehrenfest derivative coupling

$$\vec{F}(\mathbf{q}) = \sum_{st} c_s^*\vec{D}_{st}(\mathbf{q})c_t = 0. \tag{46}$$

Thus by using a diabatic electronic basis, the equations of motion can be written as

$$i\dot{A}_k = \sum_{ij} S^{-1}_{ki}\left(H^N_{ij} - i\tau_{ij}\right)A_j, \tag{47}$$

$$i\dot{\lambda}_{\beta k} = \sum_{\alpha ij} C^{-1}_{\beta k\alpha i}\rho_{ij}\left(H^{N(\alpha 0)}_{ij} - \sum_{lm} S^{(\alpha 0)}_{il}S^{-1}_{lm}H^N_{mj}\right), \tag{48}$$

$$i\dot{c}_s = \sum_t \left(H_{\mathrm{el},st}(\mathbf{q}) - \delta_{st}V(\mathbf{q})\right)c_t, \tag{49}$$

with nuclear Hamiltonian

$$H^N_{ij} = \langle g_i|T_N g_j\rangle + \langle g_i|V|g_j\rangle \tag{50}$$

and Ehrenfest potential

$$V = \sum_{st} c_s^*H_{\mathrm{el},st}c_t. \tag{51}$$

In Sec. III, we discuss how the Qu-Eh equations of motion can be implemented in a practical direct dynamics scheme.

III. IMPLEMENTATION: EHRENFEST INTERFACE TO A DD-vMCG CODE

Equations (47)–(49) describe the Qu-Eh method used in this work. We now discuss some of the practical aspects of the implementation, in particular, regarding the Ehrenfest wavefunction propagation, the need for a diabatic basis, the computation of Ehrenfest potential energy derivatives, and their use in the equation of motion for the Gaussians (details in the supplementary material).

A. CAS-CI wavefunction propagation

In this sub-section, we discuss the practical solution of equation (49). By integrating the time-dependent Schrödinger equation and discretizing time, assuming a constant electronic Hamiltonian over a time step, one obtains

$$\begin{aligned}\psi(\mathbf{r}, t_n; \mathbf{q}(t_n)) &= \exp\left(-\frac{i}{\hbar}H_{el}(\mathbf{r}; \mathbf{q}(t_n))\cdot(t_n - t_{n-1})\right) \\ &\quad \times\psi(\mathbf{r}, t_{n-1}; \mathbf{q}(t_{n-1})).\end{aligned} \tag{52}$$

In our current implementation, the time-dependent electronic wavefunction ψ is expanded in the basis of CSFs. By gathering the expansion coefficients $c_s(t_n)$ at time t_n in the vector $C(t_n)$,

$$C(t_n) = \begin{pmatrix} c_1(t_n) \\ \vdots \\ c_s(t_n) \\ c_t(t_n) \\ \vdots \end{pmatrix}. \tag{53}$$

Equation (52) using the matrix notation reads as

$$C(t_n) = \exp\left(-\frac{i}{\hbar}\mathbf{H}_e(t_n)\cdot(t_n - t_{n-1})\right)C(t_{n-1}). \tag{54}$$

Thus, the CI vector is being propagated in discretized steps, with the orbital coefficients remaining constant.

The initial Ehrenfest wavefunction is formed from approximate diabatic states (discussed in Subsection III B) within the electronic structure code via use of localized orbitals[23] (discussed below). After nuclear propagation in the DD-vMCG code, upon returning to the electronic structure code, the overall electronic wavefunction at the new geometry is determined by propagation from the previous geometry at the previous time step [Eq. (49)]. This is in contrast to a conventional DD-vMCG computation where the electronic wavefunctions of each electronic state is determined by the geometry alone (i.e., the result of "single point" calculations at that geometry and not a result of propagation from the previous geometry). As a consequence, in Qu-Eh the potential energy surface is time-dependent—one can pass through the same geometry and have a different electronic wavefunction. This again is in contrast to DD-vMCG where the adiabatic potentials at a given geometry are always the same.

B. Diabatic states approximation

As discussed in Sec. II, there is a non-adiabatic coupling term in the Ehrenfest equations that couples states s and t, via different gwp g_i. If one uses a full CI basis, then one has the freedom to localize the orbitals since the full CI energy is invariant to transformations of the active orbitals amongst themselves. These localized orbitals do not change (approximately) with geometry, hence configuration state functions constructed from localised orbitals constitute a (quasi-)diabatic basis, and this coupling term can be neglected. We have recently demonstrated[23] this in the ionization of the σ bonding orbitals in glycine, where we were able to maintain the diabatic states over an initial sample of geometries. This method has been used in our applications to be discussed subsequently.

C. Hamiltonian matrix elements and energy derivatives

To solve the equations of motion, one needs the nuclear Hamiltonian matrix [Eq. (50)] and its derivatives. While the nuclear kinetic energy operator matrix elements have simple analytical expressions in rectilinear normal mode coordinates, the electronic Hamiltonian operator matrix elements cannot *a priori* be written as a finite expansion unless some further assumptions are used. In practice, a local harmonic approximation (LHA) of the coupled potential energy surfaces is used. In the traditional DD-vMCG method, electronic structure calculations are performed using a quantum chemistry package to compute the adiabatic energies, gradients, and Hessians for *all* electronic states considered at the center of each gwp. After a diabatisation procedure,[22] second-order expansions of the diagonal and off-diagonal elements of the electronic Hamiltonian matrix are obtained in the diabatic basis, around the center of each gwp. Here, the implementation of Qu-Eh follows a similar general structure but with key differences. The energy and first and second derivatives are computed for the superposition state rather than computing derivatives separately for each of the individual states of the superposition. These derivatives are then used in the DD-vMCG-like equations of motion for nuclear propagation [Eqs. (47) and (48)]. The usual transformation in DD-vMCG of two or more adiabatic states to diabatic states (diabatization) is avoided in Qu-Eh as we only have a single time-dependent electronic state, the Ehrenfest state.

The LHA to the Ehrenfest potential [Eq. (51)] reads

$$V(\mathbf{q}) = V^l + \mathbf{G}^l\cdot(\mathbf{q}-\mathbf{q}^l) + \frac{1}{2}(\mathbf{q}-\mathbf{q}^l)^\dagger\cdot\mathbf{H}^l\cdot(\mathbf{q}-\mathbf{q}^l), \tag{55}$$

where $V^l, \mathbf{G}^l$, and $\mathbf{H}^l$ are the zeroth, first, and second derivatives evaluated at q^l,

$$V^l = V(\mathbf{q}^l), \mathbf{G}^l = \frac{\mathrm{dV}(\mathbf{q})}{\mathrm{d}\mathbf{q}}|_{\mathbf{q}^l}, \mathbf{H}^l = \frac{\mathrm{d}^2V(\mathbf{q})}{\mathrm{d}\mathbf{q}^2}|_{\mathbf{q}^l}. \tag{56}$$

Making use of the LHA, the expressions of the nuclear Hamiltonian matrix elements and its derivatives in the basis of gwp are given in the supplementary material. Giving the full form of the LHA to the Hamiltonian here would be a distraction. The most important point is that the (Hamiltonian) elements contain the first and second energy derivatives of the Ehrenfest potential,[6,7]

$$\mathrm{G}^l_\alpha = \frac{\mathrm{dV}(\mathbf{q})}{\mathrm{dq}_\alpha}|_{\mathbf{q}^l}\ \mathrm{H}^l_{\alpha\beta} = \frac{\mathrm{d}^2V(\mathbf{q})}{\mathrm{dq}_\alpha\mathrm{dq}_\beta}|_{\mathbf{q}^l}. \tag{57}$$

The only feasible method for computing these quantities is the so-called analytical derivative method, where one writes down the energy expression and differentiates it term by term. We give a brief summary here and a full development in the supplementary material.

The present work makes use of a Complete Active Space Configuration Interaction (CASCI) wavefunction (similar to CASSCF except that neither the orbitals nor CI coefficients are optimized). Since neither the orbitals nor CI coefficients are optimized, we need the complete development as given in the work of Almlöf and Taylor.[20] In these equations, one needs first and second derivatives with 3 types of variables (see the supplementary material) in addition to the gradient of the energy due to the change in the molecular Hamiltonian with nuclear geometry (the Hellmann-Feynman term): the orthogonal rotation of the orbitals among themselves as one displaces

the geometry,**C**, the orthogonal rotation of the CI eigenvectors among themselves as one displaces the geometry, and **Y**, the re-orthogonalization of the orbitals as one displaces the geometry. In CASSCF, only the latter is required.

For both gradients and second derivatives, the coupled perturbed equations have to be solved for each nuclear displacement (as discussed in the supplementary material). These equations are similar to the CASSCF coupled perturbed equations[24] except that the CI vector rotation coefficients correspond to rotations between the Ehrenfest vector and its orthogonal complement.

To summarize, in Qu-Eh dynamics, a LHA of the potential energy surface is used. Therefore, the computation of the Hamiltonian matrix elements requires the energy derivatives of the electronic wavefunction, the gradient, and the Hessian. In our current implementation, the CASCI energy derivatives are computed using the methods of Almlöf and Taylor.[20]

Our practical implementation of Qu-Eh has been made in a development version of Gaussian,[25] and uses the CASSCF formulation of the Ehrenfest method described by Vacher *et al.*[18,19] The gradients and Hessian are then passed to the Quantics quantum dynamics code[26] for a single state DD-vMCG propagation. In Qu-Eh, one requires a full computation of the gradient and Hessian for the general case where the wavefunction is not optimized.[19] At each step of the Ehrenfest algorithm for electronic motion, one solves the TDSE for nuclear motion using moving Gaussians, rather than using classical trajectories. Conceptually, this is simply Ehrenfest with quantum nuclear motion. The main approximations lie in the LHA used in DD-vMCG itself and the approximations of the Ehrenfest method.[19]

D. Summary of approximations in Qu-Eh

The Qu-Eh method allows one to carry out approximate quantum dynamics calculations with a method where the electronic wavefunction propagation and the nuclear propagation problems are treated separately. In Qu-Eh, an electronic Ehrenfest wavefunction is formed and propagated in time. The derivatives of this wavefunction are used in the DD-vMCG equations of motion for a single state (time dependent potential energy surface). The only additional approximation in the Qu-Eh method is the neglect of a non-adiabatic coupling term, as described above. This approximation can be justified by the use of (quasi-)diabatic states such that the coupling is approximately zero. Here, we use localised orbitals to construct our CSFs, therefore forming these states and allowing us to neglect the coupling.

The use of an Ehrenfest superposition state means that the DD-vMCG equations "see" only 1 state. The diabatization problem in DD-vMCG is thus moved to the electronic structure computation in Qu-Eh as discussed above. In Qu-Eh, only one electronic structure computation is required in contrast to DD-vMCG where one needs a full electronic structure computation for each adiabatic state. Of course the price to pay is that in Qu-Eh, the gradients and Hessian are more difficult to compute.

There is an additional issue in Qu-Eh: the integration required in the quantum dynamics is more difficult than in DD-vMCG, as we discuss in Sec. IV.

IV. RESULTS AND DISCUSSION

In this section, we will give three demonstrations of the application of the Qu-Eh method to the problem of charge migration.[27–34] Direct quantum dynamics methods are of particular interest in such problems because electronic and nuclear motion may not be synchronous, (e.g., charge migration in cations[35]). Charge transfer corresponds to a chemical reaction path (i.e., moving nuclei), in which a localized charge moves from one location to another as a consequence of nuclear motion: The nuclear and electronic motion are synchronized in the usual Born-Oppenheimer picture. This is to be contrasted with charge migration where one has a non-stationary electronic wave function (coherent superposition of electronic states resulting in electron dynamics) in which one has oscillatory charge migration between two localized sites. The electron and nuclear motion can be asynchronous. We have studied several examples. These include allene,[21] paraxylene, modified bismethylene-adamantane[36,37] norbornadiene cations,[38] and 2-phenyl-ethyl-amine (PEA) and 2-phenylethyl-*N*,*N*-dimethylamine (PENNA) cations.[39] The central theoretical question is whether or not charge migration persists long enough to be observed in attosecond spectroscopy.[40–43]

In the computations reported in this section, a CASSCF (N-1,N/2)/6-31g* active space was used, where N is the number of active electrons in the neutral species. The initial conditions corresponded to the creation of a localized hole at the equilibrium geometry except for allene where the terminal methylenes were rotated 45°.

There are two aspects of the initial conditions for nuclear dynamics: (1) the sampling method (momentum or position) and (2) widths of the Gaussian basis functions. The DD-vMCG method gives identical results whether one uses momentum or position sampling. However, especially for Qu-Eh, the momentum sampling method is preferred because all the gwp start at exactly the same nuclear geometry, which reduces numerical errors in the integration at the beginning of a simulation. However, because of the delicate nature of the integration in the region of turning points in electron dynamics, we were forced to use narrower Gaussian basis functions in Qu-Eh. This means that the initial wavepacket is narrower than it would otherwise be.

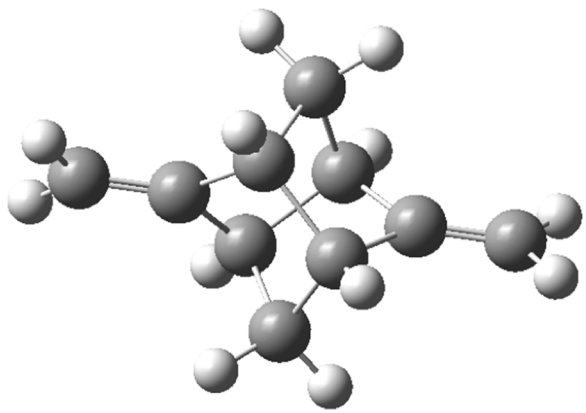

FIG. 1. Modified bismethylene-adamantane BMA.

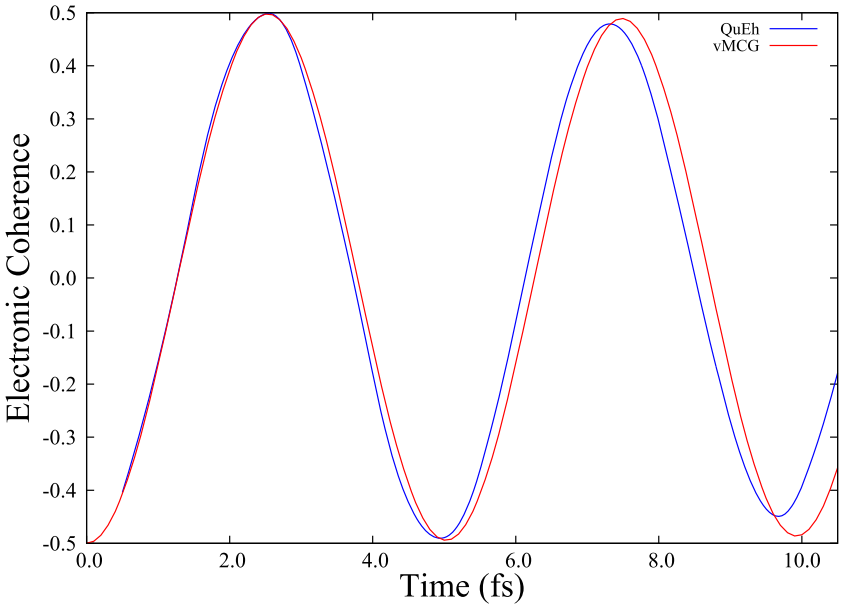

FIG. 2. Electronic coherence in BMA using DD-vMCG (red line) and Qu-Eh (blue). Both simulations used 36 gwp with initial momentum distribution. The Gaussian widths were set to 0.25 rather than 0.707, which would correspond to the width of the neutral ground-state vibrational wavefunction.

The requirement for narrower widths to allow the integration is an empirical observation and is not a fundamental requirement of the method. The problem is due to the wavepacket contracting at the turning points. The basis functions thus move into a dense formation in phase space, leading to large overlaps with resulting singularities in the inverted overlap matrix required in the basis function propagation. Such problems are common to Gaussian wavepacket based methods and improved numerical techniques will be required to deal with them.

It should be noted that the coordinates used for the dynamics are dimensionless mass-frequency scaled normal modes. Thus the widths do not have units.

A. Comparison of charge migration in BMA using DD-vMCG and Qu-Eh

We begin with a comparison of DD-vMCG vs Qu-Eh for BMA[36,37] (modified bismethylene-adamantane; see Fig. 1). In Fig. 2, we show the electronic coherence as a function of time for BMA where the hole is created in the C=CH_2 moiety. The starting conditions for DD-vMCG and Qu-Eh were identical; however, the initial nuclear wave packets (for both DD-vMCG and Qu-Eh) had narrower widths, 0.25 rather the usual 0.707, which represents a vibrational ground state in the harmonic approximation. This was necessary to maintain energy conservation at turning points in the electron dynamics. It can be seen that for short times, the agreement between DD-vMCG and Qu-Eh is acceptable. At longer times, the two approaches will differ because of different approximations in each method (e.g., the diabatization algorithm in DD-vMCG).

The convergence of the Qu-Eh itself is illustrated in Fig. 3. Here we show 36 gwp and 48 gwp Qu-Eh simulations. As noted above, in the Qu-Eh computations, the initial nuclear wave packets had narrower widths than usual. We also show our 17 gwp DD-vMCG (labeled vMCG), with the width set to

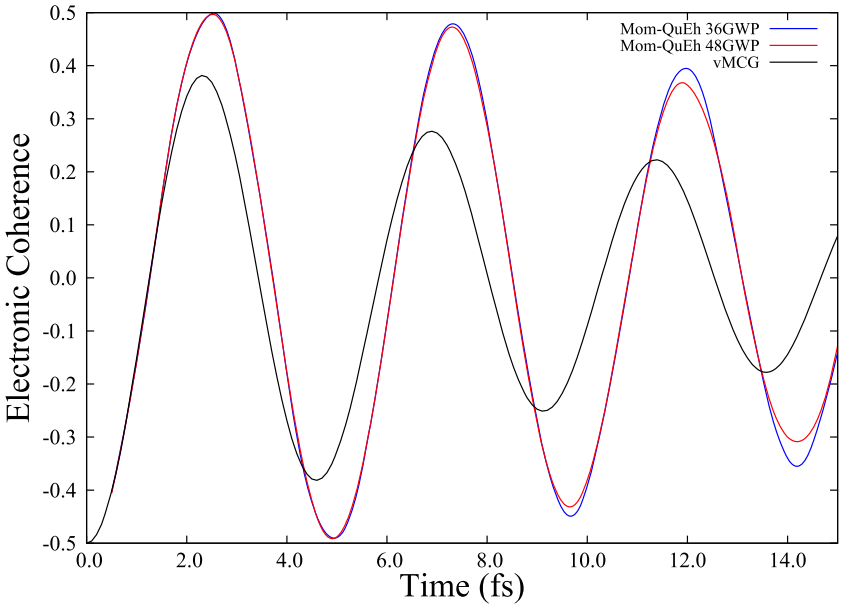

FIG. 3. Electronic coherence in BMA using DD-vMCG (black line) and Qu-Eh (blue 36 gwp and red 48 gwp). For the Qu-Eh simulations, the Gaussian widths were set to 0.25 rather than 0.707. The DD-vMCG (black line) corresponds to the DD-vMCG data published previously[36] which had the Gaussian widths set to 0.707 and used position sampling. As stated in the text, position or momentum sampling leads to identical results for vMCG.

0.707, which were originally published elsewhere.[36] (Note that position sampling was used for those simulations, although for DD-vMCG, position and momentum sampling yields identical results.) Because the initial nuclear wavepacket width is about 2.8 times narrower in the Qu-Eh simulations than in the DD-vMCG simulation, one can see that while the two simulations are in qualitative agreement, however, the decoherence in Qu-Eh is slower ($t_{1/2}$ = 18 fs) than DD-vMCG ($t_{1/2}$ = 6 fs), as could be expected from the decreased width of the nuclear wavepacket.

The computation time for Qu-Eh and DD-vMCG is dominated by the cost of the electronic structure computation at each time step. For Qu-Eh, there is only ever one electronic structure computation per time step irrespective of the number of adiabatic states involved.

B. Applications to allene and $HCCI^+$

We now illustrate the application of Qu-Eh for two examples of charge migration. For allene, we wish to illustrate the situation for very large amplitude nuclear motion (conformation change) passing near a conical intersection. By contrast, the $HCCI^+$ system involves a Renner-Teller degenerate $^2\Pi$ state (theory and experiment for this species have been discussed by Wörner *et al.*[35]).

We consider allene first. In Fig. 4, we show the spin density as a function of time on a terminal methylene for allene. Allene is a two-level problem which we have studied previously.[21] When we create a hole at a terminal methylene in allene at a 45° twisted geometry, we see that (inset Fig. 4) oscillatory charge migration is accompanied by a rotation toward 90°, where we pass close to a conical intersection and the charge migration collapses because of a zero energy gap at 10 fs and then resumes. This feature is also illustrated in Fig. 5 where we show the results for a single gwp. In Fig. 5(a),

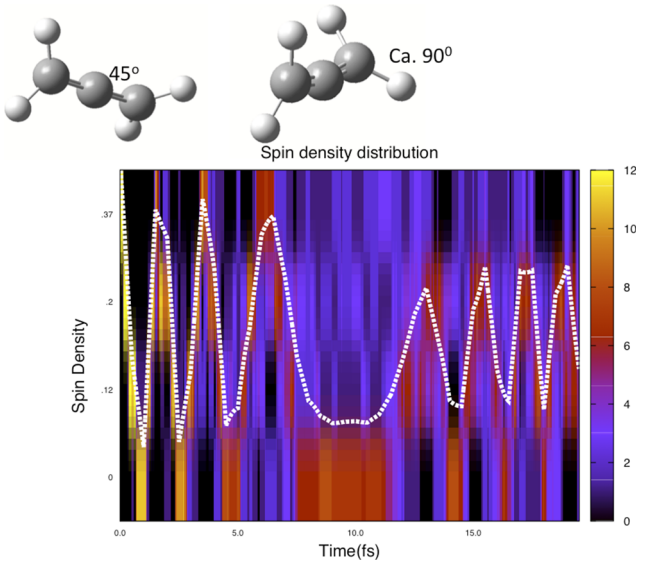

FIG. 4. Terminal Methylene Spin Density in Allene with an initial geometry with a 45° twist. Computation using 12 gwp and run for 20 fs. Dotted white line is average spin density. Colour bands show population spread across trajectories—legend on rhs. of figure showing purple is large spread in data, while yellow shows all trajectories are co-incident, i.e., all have same spin density. (See Fig. 5 for the energy gap versus time for the 1 gwp results.)

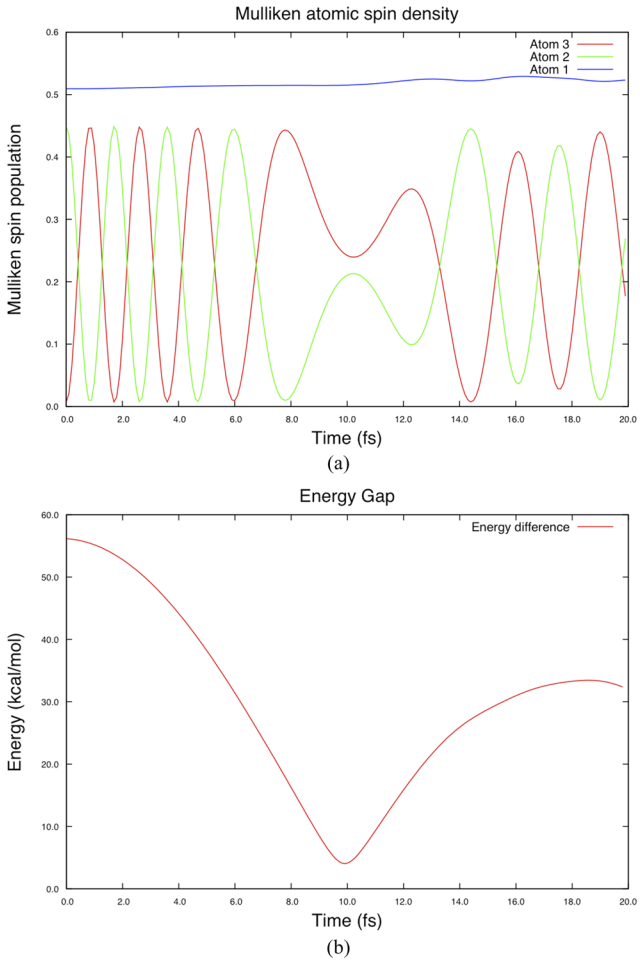

FIG. 5. Allene spin density (a) and energy gap (b) for 1 gwp.

we have plotted the spin densities on all 3 atoms. Atoms 2 and 3 are the terminal methylenes, while atom 1 is the central carbon. One can see that the spin densities become equal at approximately 10 fs. In Fig. 5(b), we show the energy gap of the adiabatic states which comes close to zero at 10 fs. The main conclusion is that the Qu-Eh method seems to be able to describe charge migration including passage near a conical intersection.

We should mention here that the details of the charge oscillation are only qualitatively similar to the previous DD-vMCG calculations of Spinlove *et al.*[21] In the earlier computations, the surfaces were for the higher lying doubly degenerate cation state and the computational method was different [Outer Valence Greens Function (OVGF) instead of CAS]. The charge oscillations had a different period and fast damping was observed. In Fig. 4, we can see that the electronic coherence recovers even after the passage near a conical intersection and the oscillations seem to increase their amplitude after that.

We turn now to the electron dynamics on the iodine atom in $HCCI^+$. In this system, we have a Renner-Teller degeneracy. In Fig. 6, we show the data for the 4-state Qu-Eh computation on $HCCI^+$ for comparison with the theoretical and experimental results of Wörner *et al.*[35] Our initial conditions correspond to the creation of a hole in one of the 2 pπ orbitals on the I atom. We use a CAS space spanning 7 electrons and 4 orbitals. This problem involves 2 pairs of degenerate $^2\Pi$ states which would

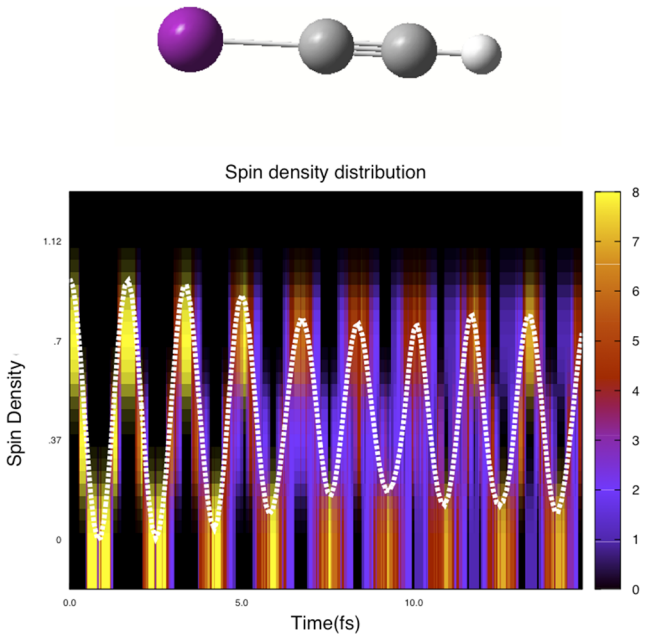

FIG. 6. Iodine spin density $HCCI^+$. Legend is the same as for Fig. 4.

require 4 electronic structure computations in DD-vMCG. In Fig. 6, we again see oscillatory charge migration to the C atoms with a frequency of 1.3 fs. In the experiments of Wörner *et al.*,[35] they observed an oscillation frequency of 1.85 fs. The coupled nuclear motion is mainly bending, which manifests itself in the change in amplitude and frequency seen in Fig. 6.

V. CONCLUSIONS

We have shown that a method (Qu-Eh), which corresponds to the Ehrenfest approach coupled to a full quantum nuclear dynamics approach (single state DD-vMCG as implemented in the Quantics code), is a useful practical approach for multi-state quantum dynamics. We have tested the method in the case where electronic and nuclear motion is asynchronous. DD-vMCG uses a local harmonic representation, so the first and second derivatives of the time-dependent potential must be computed. The method appears to be stable even in difficult cases where one passes close to a degeneracy and in a Renner-Teller linear molecule.

Our purpose in this paper was to demonstrate the applicability of Qu-Eh to charge migration problems. The Qu-Eh method is stable enough to study coherent electron dynamics on a sub-10 fs time scale and thus can be used for problems relevant to the expanding field of attosecond science.

SUPPLEMENTARY MATERIAL

See supplementary material for Energy Derivatives and the Hamiltonian in the LHA approximation.

ACKNOWLEDGMENTS

The authors are grateful for financial support from Gaussian, Inc. All calculations were run using the Imperial College Research Computing Service, DOI: 10.14469/hpc/2232.

[1] B. Lasorne, G. A. Worth, and M. A. Robb, Wiley Interdiscip. Rev.: Comput. Mol. Sci. **1**(3), 460–475 (2011).
[2] F. Krausz and M. Ivanov, Rev. Mod. Phys. **81**(1), 163–234 (2009).
[3] G. A. Worth, M. A. Robb, and B. Lasorne, Mol. Phys. **106**(16-18), 2077–2091 (2008).
[4] F. Gatti, *Molecular Quantum Dynamics* (Springer, Heidelberg, 2014).
[5] G. W. Richings, I. Polyak, K. E. Spinlove, G. A. Worth, I. Burghardt, and B. Lasorne, Int. Rev. Phys. Chem. **34**(2), 269–308 (2015).
[6] B. Lasorne, M. J. Bearpark, M. A. Robb, and G. A. Worth, Chem. Phys. Lett. **432**(4-6), 604–609 (2006).
[7] B. Lasorne, M. A. Robb, and G. A. Worth, Phys. Chem. Chem. Phys. **9**(25), 3210–3227 (2007).
[8] M. Ben-Nun and T. J. Martinez, Adv. Chem. Phys. **121**, 439–512 (2002).
[9] B. G. Levine, J. D. Coe, A. M. Virshup, and T. J. Martinez, Chem. Phys. **347**(1-3), 3–16 (2008).
[10] A. Abedi, N. T. Maitra, and E. K. U. Gross, J. Chem. Phys. **137**(22), 22A530 (2012).
[11] A. Abedi, N. T. Maitra, and E. K. U. Gross, Phys. Rev. Lett. **105**(12), 123002 (2010).
[12] F. Agostini, S. K. Min, A. Abedi, and E. K. U. Gross, J. Chem. Theory Comput. **12**(5), 2127–2143 (2016).
[13] L. S. Cederbaum, J. Chem. Phys. **138**(22), 224110 (2013).
[14] D. V. Makhov, W. J. Glover, T. J. Martinez, and D. V. Shalashilin, J. Chem. Phys. **141**(5), 054110 (2014).
[15] K. Saita and D. V. Shalashilin, J. Chem. Phys. **137**(22), 22A506 (2012).
[16] D. V. Shalashilin, J. Chem. Phys. **132**(24), 244111–244122 (2010).
[17] C. Symonds, J. A. Kattirtzi, and D. V. Shalashilin, J. Chem. Phys. **148**(18), 184113 (2018).
[18] M. Vacher, M. J. Bearpark, and M. A. Robb, Theor. Chem. Acc. **135**(8), 187 (2016).
[19] M. Vacher, D. Mendive-Tapia, M. J. Bearpark, and M. A. Robb, Theor. Chem. Acc. **133**, 1505 (2014).
[20] J. Almlöf and P. R. Taylor, Int. J. Quantum Chem. **27**(6), 743–768 (1985).
[21] K. E. Spinlove, M. Vacher, M. Bearpark, M. A. Robb, and G. A. Worth, Chem. Phys. **482**, 52–63 (2017).
[22] G. W. Richings and G. A. Worth, J. Phys. Chem. A **119**(50), 12457–12470 (2015).
[23] I. Polyak, A. J. Jenkins, M. Vacher, M. E. F. Bouduban, M. J. Bearpark, and M. A. Robb, Mol. Phys. **116**, 2474 (2018).
[24] N. Yamamoto, T. Vreven, M. Robb, M. Frisch, and H. Schlegel, Chem. Phys. Lett. **250**(3-4), 373–378 (1996).
[25] M. J. Frisch, G. W. Trucks, H. B. Schlegel, G. E. Scuseria, M. A. Robb, J. R. Cheeseman, G. Scalmani, V. Barone, G. A. Petersson, H. Nakatsuji, X. Li, M. Caricato, A. Marenich, J. Bloino, B. G. Janesko, R. Gomperts, B. Mennucci, H. P. Hratchian, J. V. Ortiz, A. F. Izmaylov, J. L. Sonnenberg, D. Williams-Young, F. Ding, F. Lipparini, F. Egidi, J. Goings, B. Peng, A. Petrone, T. Henderson, D. Ranasinghe, V. G. Zakrzewski, J. Gao, N. Rega, G. Zheng, W. Liang, M. Hada, M. Ehara, K. Toyota, R. Fukuda, J. Hasegawa, M. Ishida, T. Nakajima, Y. Honda, O. Kitao, H. Nakai, T. Vreven, K. Throssell, J. J. A. Montgomery, J. E. Peralta, F. Ogliaro, M. Bearpark, J. J. Heyd, E. Brothers, K. N. Kudin, V. N. Staroverov, T. Keith, R. Kobayashi, J. Normand, K. Raghavachari, A. Rendell, J. C. Burant, S. S. Iyengar, J. Tomasi, M. Cossi, J. M. Millam, M. Klene, C. Adamo, R. Cammi, J. W. Ochterski, R. L. Martin, K. Morokuma, O. Farkas, J. B. Foresman, and D. J. Fox, Gaussian Development Version, GAUSSIAN 16, Revision I.09, Gaussian, Inc., Wallingford, CT, 2016.
[26] K. Giri, G. A. Worth, G. W. Richings, I. Burghardt, M. H. Beck, A. Jäckle, and H.-D. Meyer, The QUANTICS Package, Version 1.1, 2015, University of Birmingham, Birmingham, UK, 2015.
[27] A. I. Kuleff, S. Lunnemann, and L. S. Cederbaum, Chem. Phys. **414**, 100–105 (2013).
[28] D. Mendive-Tapia, M. Vacher, M. J. Bearpark, and M. A. Robb, J. Chem. Phys. **139**(4), 044110 (2013).
[29] L. Belshaw, F. Calegari, M. J. Duffy, A. Trabattoni, L. Poletto, M. Nisoli, and J. B. Greenwood, J. Phys. Chem. Lett. **3**(24), 3751–3754 (2012).
[30] F. Remacle and R. D. Levine, Z. Phys. Chem. **221**(5), 647–661 (2007).
[31] A. I. Kuleff, S. Lünnemann, and L. S. Cederbaum, J. Phys. Chem. A **114**(33), 8676–8679 (2010).
[32] S. Lünnemann, A. I. Kuleff, and L. S. Cederbaum, J. Chem. Phys. **129**(10), 104305–104317 (2008).
[33] S. Lünnemann, A. I. Kuleff, and L. S. Cederbaum, Chem. Phys. Lett. **450**(4-6), 232–235 (2008).
[34] A. I. Kuleff and L. S. Cederbaum, Chem. Phys. **338**(2-3), 320–328 (2007).

[35]H. J. Wörner, C. A. Arrell, N. Banerji, A. Cannizzo, M. Chergui, A. K. Das, P. Hamm, U. Keller, P. M. Kraus, E. Liberatore, P. Lopez-Tarifa, M. Lucchini, M. Meuwly, C. Milne, J. E. Moser, U. Rothlisberger, G. Smolentsev, J. Teuscher, J. A. van Bokhoven, and O. Wenger, Struct. Dyn. **4**(6), 061508 (2017).
[36]M. Vacher, M. J. Bearpark, M. A. Robb, and J. P. Malhado, Phys. Rev. Lett. **118**(8), 083001 (2017).
[37]M. Vacher, F. E. A. Albertani, A. J. Jenkins, I. Polyak, M. J. Bearpark, and M. A. Robb, Faraday Discuss. **194**, 95–115 (2016).
[38]A. J. Jenkins, M. Vacher, R. M. Twidale, M. J. Bearpark, and M. A. Robb, J. Chem. Phys. **145**(16), 164103 (2016).
[39]A. J. Jenkins, M. Vacher, M. J. Bearpark, and M. A. Robb, J. Chem. Phys. **144**(10), 104110 (2016).
[40]M. Vacher, L. Steinberg, A. J. Jenkins, M. J. Bearpark, and M. A. Robb, Phys. Rev. A **92**(4), 040502 (2015).
[41]F. Lepine, M. Y. Ivanov, and M. J. J. Vrakking, Nat. Photonics **8**(3), 195–204 (2014).
[42]F. Frank, C. Arrell, T. Witting, W. A. Okell, J. McKenna, J. S. Robinson, C. A. Haworth, D. Austin, H. Teng, I. A. Walmsley, J. P. Marangos, and J. W. G. Tisch, Rev. Sci. Instrum. **83**(7), 071101 (2012).
[43]M. F. Kling and M. J. J. Vrakking, Annu. Rev. Phys. Chem. **59**, 463–492 (2008).